

# Single-molecule chemical reactions on DNA origami

Niels V. Voigt<sup>1,2</sup>, Thomas Tørring<sup>1,2</sup>, Alexandru Rotaru<sup>1,2</sup>, Mikkel F. Jacobsen<sup>1,2</sup>, Jens B. Ravnsbæk<sup>1,2</sup>, Ramesh Subramani<sup>1,3</sup>, Wael Mamdouh<sup>1,3</sup>, Jørgen Kjems<sup>1,4</sup>, Andriy Mokhir<sup>5</sup>, Flemming Besenbacher<sup>1,3</sup> and Kurt Vesterager Gothelf<sup>1,2\*</sup>

**DNA nanotechnology<sup>1,2</sup> and particularly DNA origami<sup>3</sup>, in which long, single-stranded DNA molecules are folded into pre-determined shapes, can be used to form complex self-assembled nanostructures<sup>4–10</sup>. Although DNA itself has limited chemical, optical or electronic functionality, DNA nanostructures can serve as templates for building materials with new functional properties. Relatively large nanocomponents such as nanoparticles and biomolecules can also be integrated into DNA nanostructures and imaged<sup>11–13</sup>. Here, we show that chemical reactions with single molecules can be performed and imaged at a local position on a DNA origami scaffold by atomic force microscopy. The high yields and chemoselectivities of successive cleavage and bond-forming reactions observed in these experiments demonstrate the feasibility of post-assembly chemical modification of DNA nanostructures and their potential use as locally addressable solid supports.**

We have used a rectangular  $100 \times 70 \text{ nm}^2$ , two-dimensional DNA origami structure formed by folding the single-stranded 7,249-nucleotide-long DNA genome of the bacteriophage M13mp18, using more than 200 synthetic oligonucleotides called staple strands<sup>3,14</sup>. Different functional groups of choice may be conjugated to selected staple strands and are thereby incorporated into the DNA origami scaffold at predetermined positions, with nanometre-scale precision. Readout of chemical reactions was accomplished by binding the small molecule biotin to selected staple strands in the DNA origami, and subsequently adding the protein streptavidin, which forms very strong non-covalent bonds with biotin. The formation or cleavage of individual chemical bonds results in either attachment or removal of the biotin–streptavidin complexes, which can be detected easily at nanometre-scale resolutions because the complexes appear as bright protrusions in atomic force microscopy (AFM) images of the origami scaffold<sup>15–20</sup>.

To demonstrate this principle, biotinylated staple strands for 12 specific positions in the origami scaffold were mixed with the remaining staple strands and the M13mp18 template, and annealed to allow the origami structure to self-assemble. After filtering off the excess staple strands, the solution was deposited on a mica surface<sup>3</sup>. Subsequent AFM images clearly show the rectangular DNA origami scaffold, but the small conjugated biotins are not detectable. The origamis are designed with an index of DNA dumbbells to determine which face of the origami is pointing towards the solution (Fig. 1). Rothemund observed an even distribution of face-up and face-down origamis, but we have found that 90–95% of the origamis have the chemically modified face pointing towards the solution<sup>3</sup>.

An excess of streptavidin was subsequently added to the origami scaffold to bind to the 12 biotins, and the AFM images recorded after incubation clearly reveal the appearance of 12 well-resolved streptavidin molecules positioned on top of the rectangular DNA origami scaffold. No origamis without streptavidins were observed, indicating that the few origamis with the biotin-modified face pointing down towards the surface can also bind streptavidin. Counting the streptavidin molecules associated with 80 well-formed DNA origamis revealed a yield of 84% for streptavidin–biotin binding.

Three different types of linkers were used in the above-mentioned 12 staple strands conjugated to the biotin molecule (Fig. 2a). Of the twelve linkers in Fig. 2a, four linkers contain a non-cleavable linker type A and four have linker type B, which contains a disulphide moiety that can be cleaved by reduction. The final four positions are linker type C, which contains an electron-rich 1,2-bis(alkylthio)ethene moiety, incorporated via the alkene phosphoramidite AP, shown in Fig. 2a (refs 21, 22). Linker C can be cleaved by singlet oxygen generated with light in the presence of a singlet oxygen photosensitizer (PS).

For the chemical cleavage of disulphide linker type B, we applied a solution of 1,4-dithiothreitol (DTT) to the DNA origami scaffold for 6 h. Following the chemical reaction, AFM imaging revealed an efficient cleavage of the disulphide bonds, as all the streptavidins from the positions corresponding to linker B had selectively disappeared (Fig. 2c).

For the succeeding cleavage of linker C, a solution of the singlet oxygen photosensitizer eosin ( $\lambda_{\text{max}} = 520 \text{ nm}$ ) was added to the surface with the immobilized T-patterned origami and thereafter illuminated with white light for 60 min. After irradiation, the sample was imaged again by AFM, and a complete disappearance of streptavidins in the positions corresponding to DNA conjugates containing linker C was observed (Fig. 2c).

Recognition of the formation of chemical bonds at the single-molecule level is an even greater challenge, because the location of the attachment point often remains unknown until the reaction occurs. However, within the present origami facilitated detection scheme, the exact position of the reacting functional group can be predetermined on the DNA origami template. To enable AFM imaging of the chemical reactions steps, we have linked the relevant incoming functional groups to biotin, which allows the visualization of a successful reaction process by the subsequent addition of streptavidin (see Supplementary Information for synthesis of the linkers)<sup>9</sup>. Using this strategy, we have studied the reactions of three functional groups: an alkyne, an amine and an azide, which are all commonly used for bioconjugation reactions. The azide

<sup>1</sup>Centre for DNA Nanotechnology (CDNA) at the Interdisciplinary Nanoscience Center (iNANO), Aarhus University, DK-8000 Aarhus C, Denmark,

<sup>2</sup>Department of Chemistry, Aarhus University, DK-8000 Aarhus C, Denmark, <sup>3</sup>Department of Physics and Astronomy, Aarhus University, DK-8000

Aarhus C, Denmark, <sup>4</sup>Department of Molecular Biology, Aarhus University, DK-8000 Aarhus C, Denmark, <sup>5</sup>Institute of Inorganic Chemistry, Ruprecht-Karls University, Heidelberg, Germany. \*e-mail: kvg@chem.au.dk

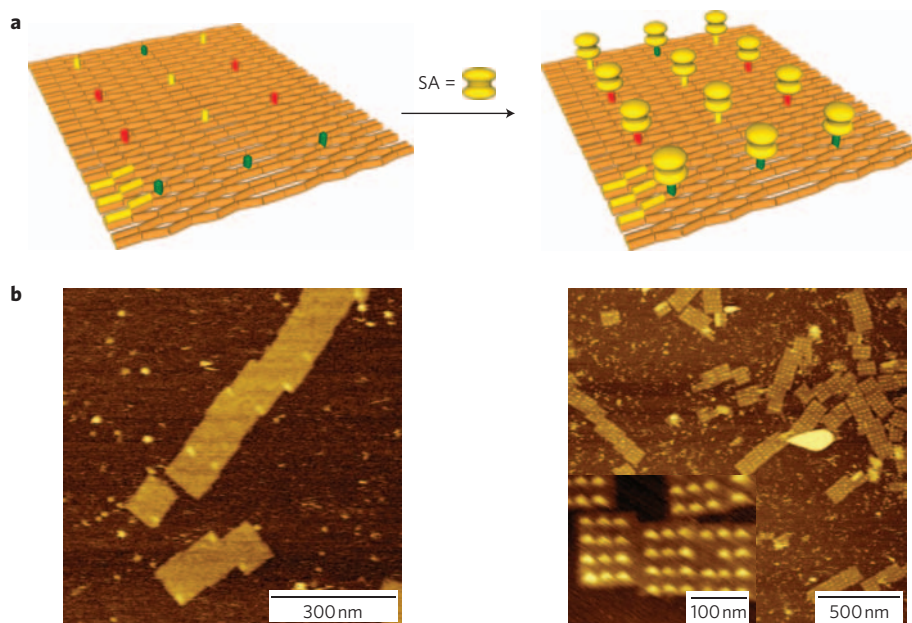


**Figure 1 | Predetermined positioning of streptavidin on a DNA origami scaffold.** **a**, Positions of index and 5'-biotinylated DNA strands on rectangular-shaped DNA origami. (Orange, rectangular origami; yellow bars, index; yellow SA, streptavidin; yellow, red and green, different linker types (see Fig. 2a)). **b**, AFM images of the biotin-modified origami with reference index in the lower left corner, and the precisely positioned streptavidin molecules on the origami surface in the lower right corner. Inset: enlarged image.

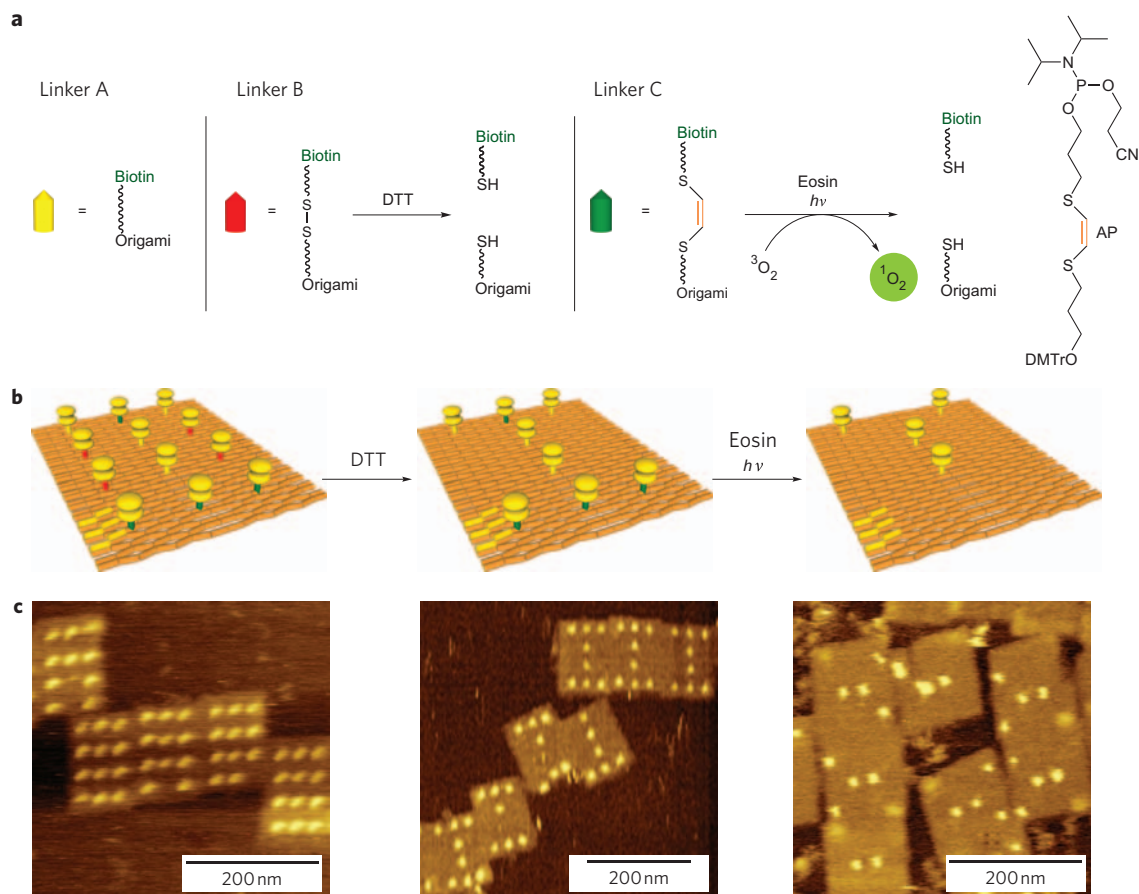


**Figure 2 | Chemical cleavage reactions on DNA origami.** **a**, Linkers A, B and C used for immobilization of biotin. Linkers B and C are cleavable. Linker B is cleaved by DTT (10 mM) and linker C by photogenerated singlet oxygen (sensitizer, eosin 100  $\mu\text{M}$ ). AP is the phosphoramidite used for the synthesis of linker C. **b**, Schematic of the arrangement of the linker-biotin-streptavidin conjugates at the DNA origami. **c**, AFM images of origamis with streptavidins arranged as the letter 'I' after disulphide cleavage, and the letter 'Y' after subsequent photochemical cleavage.

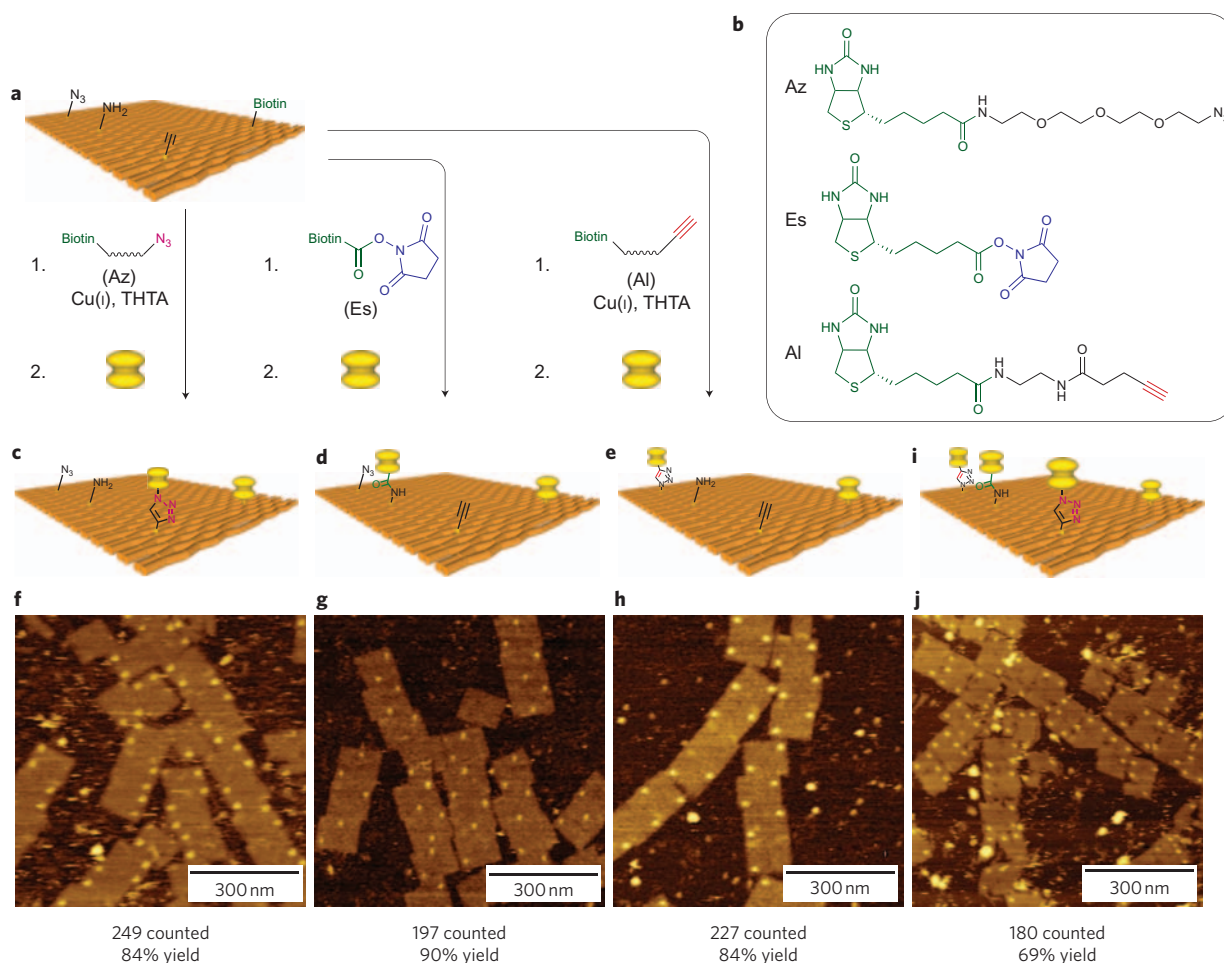


**Figure 3 | Chemical coupling reactions on DNA origami.** **a**, Model of the DNA origami scaffold incorporating a biotin reference and three functional groups (an alkyne, an amine and an azide) and their reactions with the complementary functionalities (yellow structure, streptavidin). **b**, Chemical structure of the biotin-tethered functional groups Az, Es and Al. **c–e**, Model of the expected product of the reactions with Az, Es and Al after incubation with streptavidin. **f–h**, AFM images of the respective reaction products illustrated in **c–e**, respectively. **i**, Model of the expected product after three successive reactions with Al, Es and Az. **j**, AFM imaging of the product.

can react with an alkyne and vice versa in a Huisgen–Sharpless–Meldal copper(I)-catalysed click reaction to form a triazole<sup>23,24</sup> and the amine can react with an *N*-hydroxysuccinimide activated ester (NHS-ester) to form an amide moiety (Fig. 3a). Three positions on the origami scaffold were modified with the three different functional chemical groups, and biotin was inserted at a fourth position as an internal reference (Fig. 3a). The matching chemical reactants, linked to biotin, were also synthesized (Fig. 3b). To study the reactions, the self-assembled origami structure containing all three functional groups was deposited on a mica surface under HEPES/Mg<sup>2+</sup> buffer (pH = 7.4), and all the subsequent chemical reaction steps were performed *in situ* on the surface-immobilized DNA origami scaffold at room temperature. Because of the strong interactions between the DNA origami structure and the mica surface, the adsorbed DNA scaffold resembles a solid phase, and we find that several consecutive exchanges of the solution and excess reagents can be performed without any significant degradation of the DNA origami scaffold.

The click reaction of the biotin-linked azide Az took place in the presence of the *in situ* generated copper(I)-THTA (*tris*-(1-[3-hydroxypropyl]triazolyl-4-methyl)amine) catalyst<sup>25</sup> (Fig. 3c), whereas the reaction of the biotin NHS-ester Es was performed in a slightly alkaline buffer/DMF mixture (pH = 8.3; Fig. 3d). Finally, the reaction of the biotin-linked alkyne Al was studied in the presence of the *in situ* generated copper(I)-THTA in a DMF/buffer mixture

(Fig. 3e). Each of the three reactions was performed by incubation with the reagents for 20 min. To image the products of the three separate chemical reactions, the immobilized origami samples were subsequently incubated with streptavidin for 5 min after each reaction, and imaged under liquid by AFM. The AFM images depicted in Fig. 3f–h reveal streptavidin molecules placed in predefined positions on top of the DNA origami scaffold. Based on a thorough analysis of ~250 well-defined origami structures, the yields of each of the three reactions were determined. Each protrusion observed on the DNA origami surface in a given position is the product of the covalent chemical reaction and the biotin–streptavidin interaction, and the yields of the covalent reactions are thus determined by dividing the observed yield with the ~85% efficiency of the streptavidin binding in the reference position (see Methods for further explanation and calculations). From this analysis, the reactions proceed with a yield of ~84–90%. Furthermore, we find that the reactions proceed with a high degree of chemoselectivity, because in none of the more than 600 investigated origami structures from the three reactions was any misplaced streptavidin observed. Because conventional ensemble analysis techniques cannot exclude the presence of such side reactions in bioconjugation reactions, the present novel DNA origami template scheme is clearly superior in terms of specificity.

Finally, we show that the three reactions can proceed successively on the immobilized DNA origami template with high selectivity.

Such selective conjugation of two or more different chemical groups to a biomolecular structure is often very challenging and requires two or more specific chemical reactions<sup>26</sup>. Here, the reactions were each performed for 20 min in the order of the surface groups, alkyne, amine and azide (Fig. 3i), and the sample was subsequently incubated with streptavidin. The recorded AFM images (Fig. 3j) show that a large fraction of the DNA origami remains immobilized on the surface after successive reaction and washing steps (Fig. 3i). However, a slightly higher frequency of dark spots on the individual DNA origami templates indicates some degree of degradation. To explore the reactions quantitatively, all streptavidin molecules on the well-shaped two-dimensional origami templates were assigned according to position, and of the 180 well-shaped DNA origami structures investigated, 40% contained all three streptavidin proteins in positions coinciding with the three functional groups. Because the yield also covers the three biotin-streptavidin interactions, the yield of the three reactions is determined to be 69%, corresponding to an average yield of 88% for the three individual reactions (for further information on the statistics see Methods).

In summary, we have revealed a new approach to single-molecule imaging by AFM of chemical reactions. The method offers the possibility to gain fundamental insight into covalent chemical reactions on an assembled DNA nanostructure. It has a range of interesting potential applications; for example, the ability to selectively monitor the cleavage of linker type C by singlet oxygen potentially provides an ultra-sensitive method with which to monitor singlet oxygen<sup>27</sup>. Furthermore, the local nature of the two-dimensional origami assay holds the interesting potential for monitoring singlet oxygen production and diffusion from a single sensitizer as a function of distance.

Our results demonstrate that the DNA origami structure provides a highly versatile breadboard for chemical reactions and can be used as a locally addressable solid support. In particular, it may become possible to prepare macromolecular structures by chemical reactions between functional groups placed at different pixels on the two-dimensional origami templates. This would open up a new type of chemical synthesis in which monodisperse macromolecules can be synthesized in a parallel process<sup>28,29</sup> where the selectivity is determined by the position and orientation of the molecule on the DNA scaffold, rather than by the conventional iterative synthesis and massive use of protecting groups.

Received 3 September 2009; accepted 14 January 2010;  
published online 28 February 2010

## References

- Seeman, N. C. An overview of structural DNA nanotechnology. *Mol. Biotechnol.* **37**, 246–257 (2007).
- Gothelf, K. V. & LaBean, T. H. DNA-programmed assembly of nanostructures. *Org. Biomol. Chem.* **23**, 4023–4037 (2005).
- Rothmund, P. W. K. Folding DNA to create nanoscale shapes and patterns. *Nature* **440**, 297–302 (2006).
- Qian, L. *et al.* Analogic China map constructed by DNA. *Chin. Sci. Bull.* **51**, 2973–2976 (2006).
- Andersen, E. S. *et al.* DNA origami design of dolphin-shaped structures with flexible tails. *ACS Nano* **2**, 1213–1218 (2008).
- Andersen, E. S. *et al.* Self-assembly of a nanoscale DNA box with a controllable lid. *Nature* **459**, 73–76 (2009).
- Ke, Y. *et al.* Scaffolded DNA origami of a DNA tetrahedron molecular container. *Nano Lett.* **9**, 2445–2447 (2009).
- Kuzuya, A. & Komiyama, M. Design and construction of a box-shaped 3D-DNA origami. *Chem. Commun.* 4182–4184 (2009).

- Douglas, S. M. *et al.* Self-assembly of DNA into nanoscale three-dimensional shapes. *Nature* **459**, 414–418 (2009).
- Dietz, H., Douglas, S. M. & Shih, W. M. Folding DNA into twisted and curved nanoscale shapes. *Science* **325**, 725–730 (2009).
- LaBean, T. & Li, H. Using DNA for construction of novel materials. *Nano Today* **2**, 26–35 (2007).
- Rinker, S., Ke, Y., Liu, Y., Chhabra, R. & Yan, H. Self-assembled DNA nanostructures for distance-dependent multivalent ligand–protein binding. *Nature Nanotech.* **3**, 418–422 (2008).
- Ke, Y., Lindsay, S., Chang, Y., Liu, Y. & Yan, H. Self-assembled water-soluble nucleic acid probe tiles for label-free RNA hybridization assays. *Science* **319**, 180–183 (2008).
- Chhabra, R. *et al.* Spatially addressable multiprotein nanoarrays templated by aptamer-tagged DNA nanoarchitectures. *J. Am. Chem. Soc.* **129**, 10304–10305 (2007).
- Yan, H., Park, S. H., Finkelstein, G., Reif, J. & LaBean, T. H. DNA-templated self-assembly of protein arrays and highly conductive nanowires. *Science* **301**, 1882–1884 (2003).
- Lund, K., Liu, Y., Lindsay, S. & Yan, H. Self-assembling a molecular pegboard. *J. Am. Chem. Soc.* **127**, 17606–17607 (2005).
- Park, S.-H. K. *et al.* Finite-size, fully addressable DNA tile lattices formed by hierarchical assembly procedures. *Angew. Chem. Int. Ed.* **45**, 735–739 (2006).
- Park, S.-H. *et al.* Programmable DNA self-assemblies for nanoscale organization of ligands and proteins. *Nano Lett.* **5**, 729–733 (2005).
- Kuzuya, A. *et al.* Precisely programmed and robust 2D streptavidin nanoarrays by using periodical nanometer-scale wells embedded in DNA origami assembly. *ChemBioChem* **10**, 1811–1815 (2009).
- Kuzyk, A., Laitinen, K. T. & Törmä, P. DNA origami as a nanoscale template for protein assembly. *Nanotechnology* **20**, 235305 (2009).
- Baugh, S. D. P., Yang, Z., Leung, D. K., Wilson, D. M. & Breslow, R. Cyclodextrin dimers as cleavable carriers of photodynamic sensitizers. *J. Am. Chem. Soc.* **123**, 12488–12494 (2001).
- Rotaru, A. & Mokhir, A. Nucleic acid binders activated by light of selectable wavelength. *Angew. Chem. Int. Ed.* **46**, 6180–6183 (2007).
- Tornøe, C. W., Christensen, C. & Meldal, M. Peptidotriazoles on solid phase: [1,2,3]-triazoles by regioselective copper(I)-catalyzed 1,3-dipolar cycloadditions of terminal alkynes to azides. *J. Org. Chem.* **67**, 3057–3064 (2002).
- Rostovtsev, V. V., Green, L. G., Fokin, V. V. & Sharpless, K. B. A stepwise Huisgen cycloaddition process: copper(I)-catalyzed regioselective 'ligation' of azides and terminal alkynes. *Angew. Chem. Int. Ed.* **41**, 2596–2599 (2002).
- Chan, T. R., Hilgraf, R., Sharpless, K. B. & Fokin, V. V. Polytriazoles as copper(I)-stabilizing ligands in catalysis. *Org. Lett.* **6**, 2853–2855 (2004).
- van Kasteren, I. *et al.* Expanding the diversity of chemical protein modification allows post-translational mimicry. *Nature* **446**, 1105–1109 (2007).
- Schweitzer, C. & Schmidt, R. Physical mechanisms of generation and deactivation of singlet oxygen. *Chem. Rev.* **103**, 1685–1758 (2003).
- Gothelf, K. V. *et al.* Modular DNA-programmed assembly of linear and branched conjugated nanostructures. *J. Am. Chem. Soc.* **126**, 1044–1046 (2004).
- Andersen, C. S., Yan, H. & Gothelf, K. V. Bridging one helical turn in double-stranded DNA by templated dimerization of molecular rods. *Angew. Chem. Int. Ed.* **47**, 5569–5572 (2008).

## Acknowledgements

The authors would like to thank V. Birkedal and T. LaBean for valuable comments regarding the manuscript. This work was supported by grants from the Danish National Research Foundation to the CDNA centre and the Danish Research Agency through support for the iNANO Center.

## Author contributions

N.V.V., T.T. and A.R. contributed equally to the design and execution of the experiments. M.F.J. and J.B.R. synthesized some of the organic compounds. R.S. and W.M. assisted in the AFM imaging. A.M. provided Linker C. J.K. and F.B. advised on the project. K.V.G. directed the project and co-wrote the manuscript. All authors discussed the results and commented on the manuscript.

## Additional information

The authors declare no competing financial interests. Supplementary information accompanies this paper at [www.nature.com/naturenanotechnology](http://www.nature.com/naturenanotechnology). Reprints and permission information is available online at <http://npg.nature.com/reprintsandpermissions/>. Correspondence and requests for materials should be addressed to K.V.G.